Modeling Large Phased Array Antennas Using the Finite Difference Time Domain Method and the Characteristic Basis Function Approach

(*Invited Paper*)

Nader Farahat*, Raj Mittra, and Neng-Tien Huang****
*Polytechnic University of Puerto Rico
P.O. box 192017 San Juan, PR 00919
**The Pennsylvania State University, 319 EE East
University Park, PA, 16802, USA

Abstract**–**In this paper we describe an approach for solving large phased array problems, using the Characteristic Basis Function Method (CBFM) in conjunction with the Finite Difference Time Domain (FDTD) technique. The method is especially tailored for solving large arrays that may be covered with Frequency Selective Surfaces (FSSs). Several illustrative examples are provided and the results are validated for a number of test cases. This is accomplished by comparing the results derived by using the proposed technique with those obtained via a direct simulation of the entire array on a PC cluster. Of course, the direct problem places a heavy demand on the computer resources, especially as the problem size becomes large. In contrast to the direct method, the increases in the simulation time and the burden on the computer memory are incrementally small in the present approach, as the problem size is increased from moderate to large.

I. INTRODUCTION

Numerical modeling of large but finite phased array antennas is a challenging problem because it places a heavy burden on the computer resources, especially when the array element is complex, and the antenna operates in a close proximity of an FSS radome whose period is not commensurate with that of the array. The array element is typically a microstrip patch, a Vivaldi or a waveguide, and the antenna may be covered by an FSS radome, whose elements may be patches, slots, cross-dipoles, etc., typically different from those of the array. Accurate prediction of the performance of such complex antenna systems is a very challenging problem indeed.

The Finite Difference Time Domain (FDTD) [1] method has proven to be a robust technique for modeling a wide variety of electromagnetic systems. In addition to its versatility and ability to handle complex geometries, it has the added advantage of being able to obtain the response of a device over a wide band of frequencies from a single run. Although the parallelization of the FDTD enables us to solve large problems using distributed processing, it is still desirable to reduce the solve time and memory requirements, whenever possible. Recently, the Characteristic Basis Function Method (CBFM) has been proposed as a technique for fast and accurate modeling of large structures both for scattering and radiation problems, and has been tailored for both the Method of Moments (MoM) and the FDTD [2-5]. The CBFM utilized in this work is based on the localization of the fields by using certain types of excitations to generate a set of basis functions with which to synthesize the solution to the original problems.

In this paper we extend the application of the CBFM to the problem of analyzing large phased array antennas, taking into account of the inter-element mutual coupling, which is often ignored in approximate methods—such as the pattern multiplication technique—in order to render the problem manageable. The validation is carried out by comparing the CBFM-based results with those obtained by using the parallel version of the FDTD (PFDTD) on a cluster. It should be mentioned that the use of the CBFM allows one to solve much larger problems than would be possible by using the direct method, at little or no extra cost beyond that needed to solve of a moderate-size problem, which can be conveniently handled by using the PFDTD code, because of its manageable size. In addition, we show how the discrete phase progression of antenna elements which is modeled in the FDTD has a significant effect on the accuracy of the resulting far-field patterns.

II. THE CBFM TECHNIQUE

To further explain the underlying concepts of the CBFM for arrays, we start with an example of a 21 by 21 rectangular waveguide array, shown symbolically in Fig. 1.

Fig. 1. Illustration of 21 × 21 rectangular waveguides. The picture symbolically shows the TE_{10} mode excitation in each waveguide.

Each element of the array is excited in a TE_{10} mode. The entire array is simulated by using the FDTD method and the electric field distribution at the frequency of operation in the aperture of the waveguides are derived (see Fig. 2 that shows the co-polar components). We observe that the distribution of the fields at the edges and corners differs from those in the center region. Hence, we note that the inherent assumption in the pattern multiplication approach, namely that all the elements are identical, is not really valid. Next, we investigate the case where only the center element of the same array is excited. We see from Fig. 3 that the effect of the inter-element mutual coupling is extended up to a few neighboring elements and is relatively strong in the E-plane (vertical direction) as compared to the H-plane (horizontal direction). Next, we argue that in the center region the field distribution only shifts in space (Fig. 4) as we move the location of the excitation source. We refer to these aperture distributions as the CBFs. We note that for the center region, the CBFs are relatively invariant to the location of the excitation source. Hence, we can bypass a considerable amount of computation involved in the generation of the CBFs by taking advantage of this feature. We can also use the localization approach to generate the CBFs for the edge and corner regions, and can reduce the computation time for these CBFs again by avoiding the duplicate calculations.

Once the CBFs have been constructed, we can synthesize the aperture field of the array via superposition, as shown in Fig. 5.

Assuming that the array is mounted in a metallic frame, we can assume that the fields external to the array vanish in the plane of the array. We can then perform a near-to-far-field transformation to compute the pattern of the array. If we make the further assumption that the

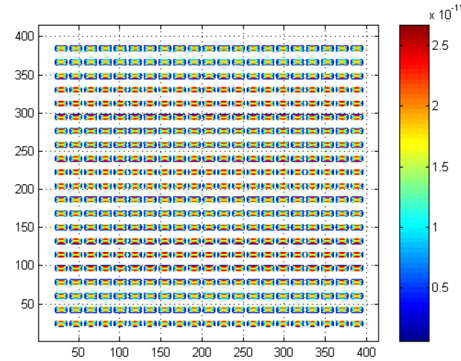

Fig. 2. Distribution of the co-polar component of the electric field in the opening of the 21 × 21 rectangular waveguides.

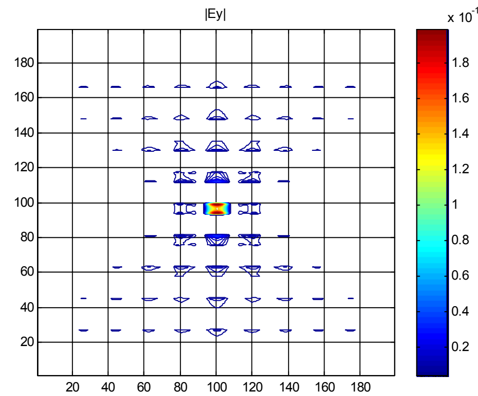

Fig. 3. Distribution of the co-polar component of the electric field in the opening of the 9 × 9 rectangular waveguides when only the center element is excited.

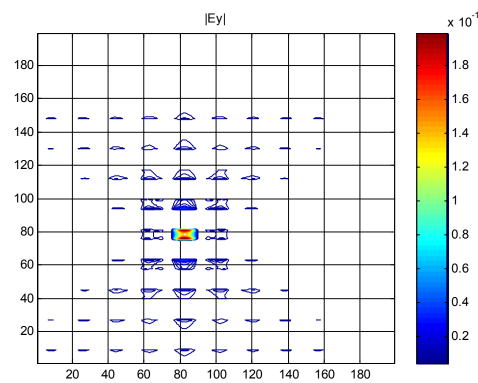

Fig. 4. Distribution of the co-polar component of the electric field in the opening of the 9 × 9 rectangular waveguides when only the next to the center element is excited.

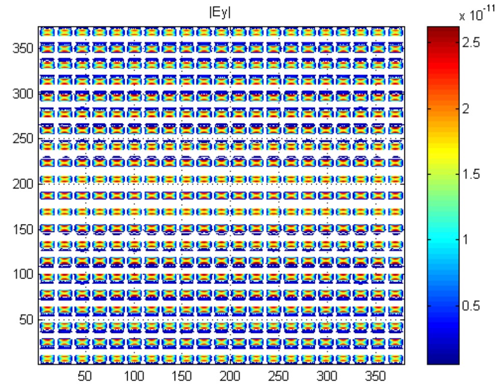

Fig. 5. Distribution of the co-polar component of the electric field in the opening of the 21 × 21 rectangular waveguides reconstructed after proper shift and superposition.

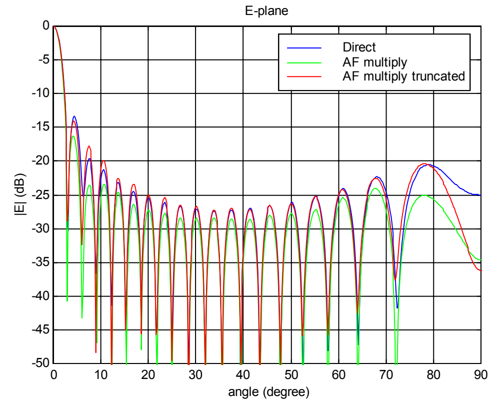

Fig. 6. E-plane far-field pattern of the 21 × 21 waveguide array obtained by using different techniques.

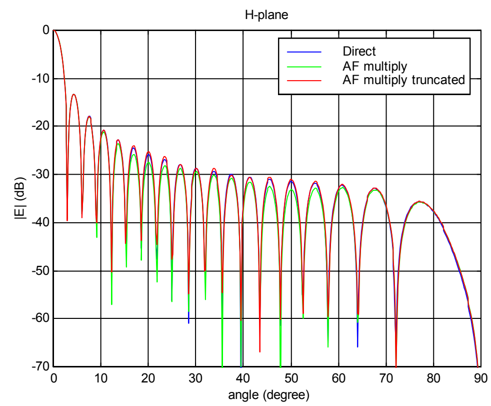

Fig. 7. H-plane far-field pattern of the 21 × 21 waveguide array obtained by using different techniques.

behavior of the aperture fields remains relatively unchanged when we move the source from one waveguide to another, even when we are close to edge, or a corner, we can construct the aperture field by simply shifting, superposing and, finally, truncating the synthesized aperture fields to within the interior of the metallic frame. The above procedure can be implemented equally well in the spectral domain by superposition of the spectral transforms of CBFs. However, at the end, it becomes necessary to perform a convolution of the resultant with a window function, which is equivalent to truncating the fields in the region external to the array aperture in the spatial domain approach. We have found that the first approach (spatial domain) is simpler to implement than its counterpart in the spectral domain.

Next, we present in Figs. 6 and 7 the far-field patterns, for the E- and H-planes, respectively, derived by using the different techniques. We see that the effect of mutual coupling is insignificant in the H-plane and that the pattern multiplication, though approximate, yields results with reasonably good accuracy in this plane. This is consistent with the results shown in Figs. 3 and 4, in which the coupling in the horizontal plane is seen to be weak. However, the pattern multiplication approach is no longer accurate in the E-plane, and the improvement in accuracy in the CBFM results over the pattern multiplication method is evident in this plane.

We now summarize the CBFM as applied to the large but finite array problems. We begin in this method with the modeling of a moderate-size array, which is only large enough to capture the mutual coupling effects associated with the excited element. Once we have derived this aperture field, we can generate the results for the larger sizes of the array by shifting, superposing and truncating the above aperture field. We mention, once again, that an extrapolation of the solution from a moderate to a large-size array only requires a trivial amount of additional computational effort and memory usage, and the accuracy of the results improves as well. These are unique and very desirable features of the CBFM, not readily found in other approaches.

III. BEAM SCANNING CASE

We now go on to show in this section that the method, described above, can be used for beam scanning as well. The only modification needed is the addition of appropriate phase shift to the CBFs to account for the progressive phase shift introduced in the array elements to enable the array to scan. To illustrate the application of the CBFM to this case, we consider the example of a 9 x 9 array of waveguides and use the procedure for synthesizing the aperture field to obtain the results for a 21 x 21 array with 60 degree progressive phase shift of the elements along the H-plane, which corresponds to an 11 degree scan. The aperture field synthesis is accomplished by simulating the 9 x 9 array when only the center region is excited, followed by aperture translation, introduction of the phase progression, superposition, truncation, etc., and, finally, the near-to-far-field transformation. Figure 8 shows the comparison of the CBFM results with that obtained by using the direct simulation of array 21 x 21 by FDTD, in which the progressive "time delay" has been added in the excitation of the elements corresponding to the 60 degree progressive phase at the frequency of interest.

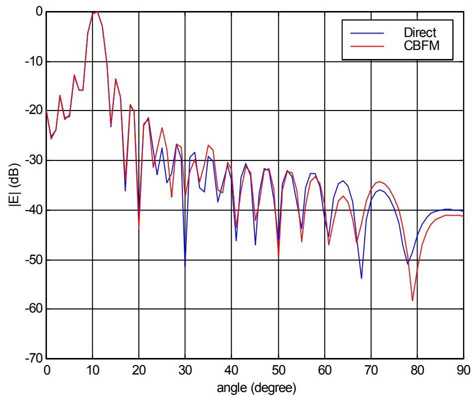

Fig. 8. H-plane far-field pattern of 21 × 21 rectangular waveguides (H-plane 60 degree progressive phase).

The difference between the direct solution and the CBFM result is evident in this case. A close examination of the source of the error reveals that it is the discretization in the time delays introduced in the FDTD excitation that is responsible for this error, and this leads us to conclude that we need to enforce the time delay more precisely in the direct method to obtain the results with the desired accuracy. To mitigate the phase error problem, we need to deliberately decrease the time step to a value smaller than that dictated by the Courant condition from stability considerations. We illustrate this fact by referring to Fig. 9, which shows the linear phase taper introduced in the FDTD simulation along the 21 elements in the H-plane (Fig 9). Next, in Fig. 10, we plot the deviation from the ideal linear phase for two cases: (i) Courant-based time-step; (ii) one-half of Courant-based time-step. We observe that decreasing the time step has the effect of reducing the error in phase shift from 10 to 4 degrees, and the resulting improvement in the corresponding the patterns is evident from Fig. 11. Figure 12 shows that the phase shift error can be further reduced by choosing smaller time steps and, as expected, this helps reduce the deviation of the pattern from the expected exponential decrease of the side lobes (see Fig. 13).

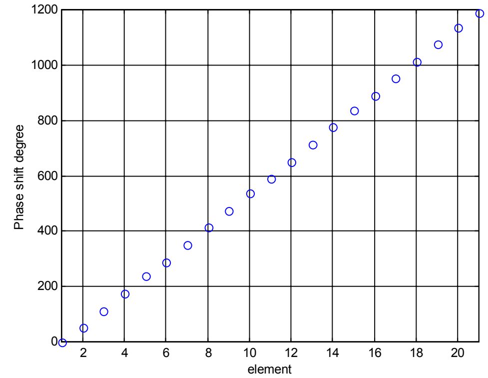

Fig. 9. Linear phase taper introduced in the FDTD simulation.

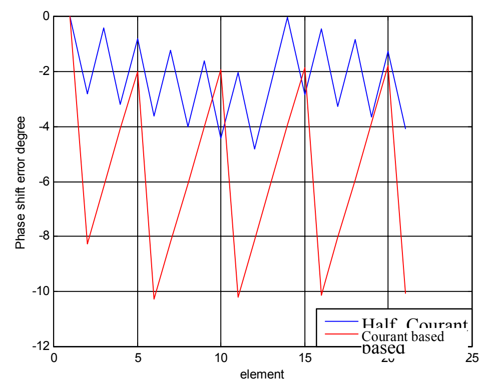

Fig. 10. Reduction of the phase errors when the time step is shortened by a factor of two from that of the Courant condition.

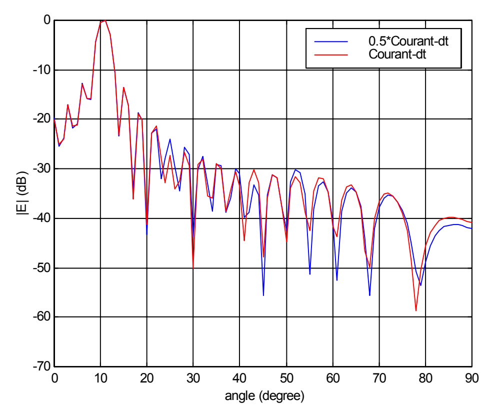

Fig. 11. Change in the Pattern with the reduction in the time step.

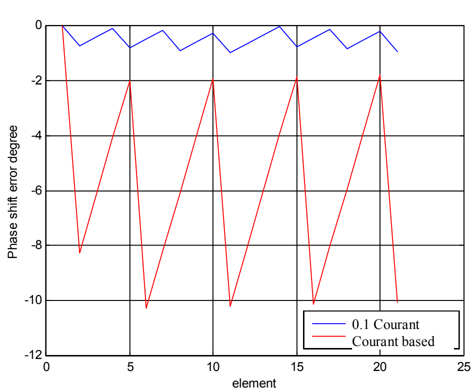

Fig. 12. Further reduction of the phase error when the time step is 0.1 of Courant condition.

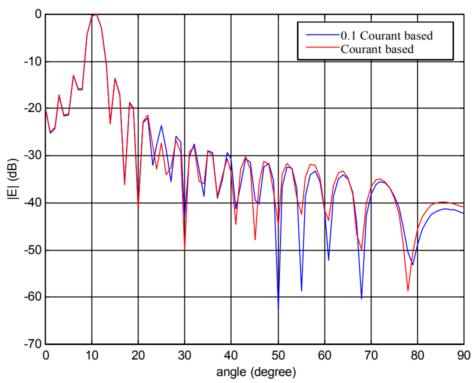

Fig. 13. Comparison between the patterns with time delay equal to 0.1 Courant condition and that obtained by using CBFM.

It is worthwhile mentioning here that it is not necessary to significantly reduce the time step--which leads to a long simulation time--if we are only interested in modeling the array single frequency at a time. This is because we can always find an adjusted time-step, which is not much smaller than the Courant-based time-step, whose integral multiple equals the required time delay, and whose use essentially eliminates the phase errors. For instance, in the previous example, we can choose a time step that equals 0.9432 of the Courant time-step so its integral multiple is exactly equal to the time delay. The maximum error between the elements then reduces to levels below a few thousandth of a degree as shown in Fig. 14, and the pattern (see Fig. 15) is identical to that obtained by using a time-step equal to a tenth of the Courant-based time step. Note that, with this modification in the direct FDTD solution, we again obtain an excellent agreement (see Fig. 16) between it and the CBFM, albeit for a fixed frequency. (The time step has to be reset as the frequency is changed in order to maintain the accuracy of the direct solution).

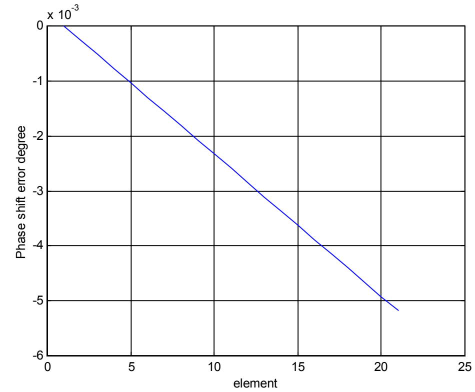

Fig. 14. Phase error for the time step of 0.9432 of Courant condition.

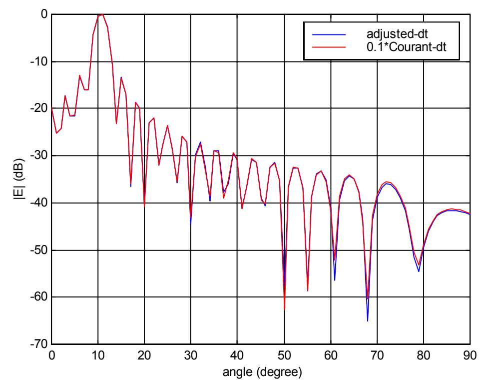

Fig. 15. Comparison between the patterns with time steps equal to 0.9432 and 0.1 Courant condition.

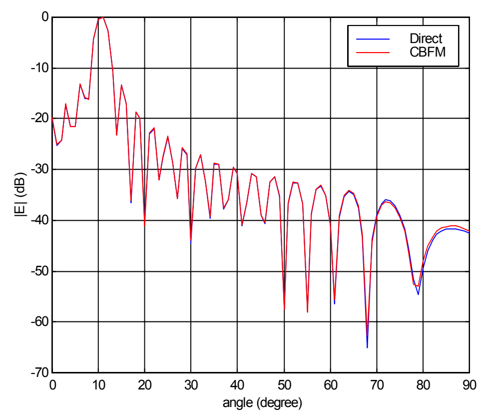

Fig. 16. Comparison between the direct H-plane pattern employing 0.9432 Courant for the time step and that generated by CBFM.

On the basis of the above study, we conclude that one has to be careful while generating the direct solution during the process of validating the CBFM result to ensure that the former is sufficiently accurate.

Of course, we realize that the above phase error problem would not exist if we were to carry out the simulation in the frequency rather than in the time domain.

Earlier we had mentioned that the CBFM technique does not suffer from the phase error because the phase shifts are introduced directly and precisely in the aperture. However there is an exception to the above statement that we should bring to the attention of the reader. The phase error may also exist in the CBFM analysis, unless the time delay is adjusted to minimize or eliminate it, when we derive the aperture basis functions by exciting a cluster of elements in the array, rather than a single one. As detailed in the next section, this type of excitation is employed, for instance, when we are modeling composite arrays, comprising of phased array antennas covered with FSS radomes, whose periods are dissimilar. For this configuration, we excite a macro-unit cell of the antenna-radome composite to generate the basis functions, and we introduce a progressive time delay for the scan case within this macro-cell. We reiterate that this error does not exist for the case of single element excitation and, more importantly, when we extend the results from a moderate array to a larger one using the CBFM, since it carries out the phase shifting artificially, independent of the FDTD simulation.

IV. COMPOSITE ARRAYS

For the last example, we apply the CBFM to a composite array structure, comprised of phased array antenna covered by an FSS radome, depicted symbolically in Fig. 17. It shows a waveguide array covered by a loop-type FSS radome, and we note that the periodicities of the two are not the same.

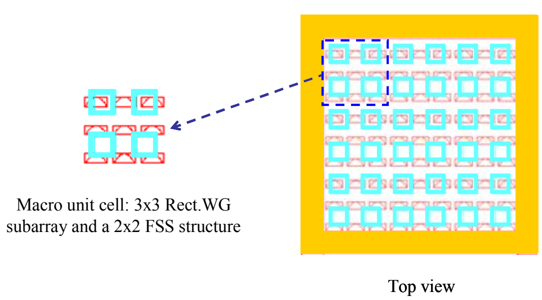

Fig. 17. Illustration of the 3 x 3 array of waveguide-with-FSS macrocell.

To tackle this problem using the CBFM, we define a macro-unit containing 3 x 3 waveguide array, covered by the 2 x 2 loop array. To implement the CBFM for this problem, we again simulate a moderate-size array of 3 x 3 macro-unit cells, and then use the result of this simulation to synthesize the aperture distribution of a larger array comprising of 441 waveguides. In the simulation of the 3 x 3 macro-unit cells we have to excite the waveguides of the center macro-unit cell in the progressive time delay in order to scan 11 degrees along the H-plane. As explained in the previous section, to achieve the required accuracy we need to adjust the time step such that an integral multiple of this step exactly equals the required time delay for the corresponding beam scan at the frequency of interest. Once again, to validate the CBFM result, we carry out a direct simulation of the entire array using a parallel FDTD code running on a cluster of computers. Similar to the previous example, we adjust the time step for the required time delay. The comparison between the two results, shown in Fig. 18, demonstrates that the CBFM results are quite accurate. We reiterate, once again, the fact that the extension to larger arrays merely requires a post-processing of the data obtained previously, and does not require additional simulation that can be time-consuming. Fig. 19 verifies the above statement and shows that the patterns obtained by CBFM and direct simulation for a 3969 waveguide array are in good agreement with each other. It goes without saying that direct simulation is very expensive to obtain for this large problem, as it requires sizable computational resources in terms of CPU time and memory. On the other hand, the CBFM can handle arbitrarily large arrays with little difficulty, and with only a slight increase in the computational burden.

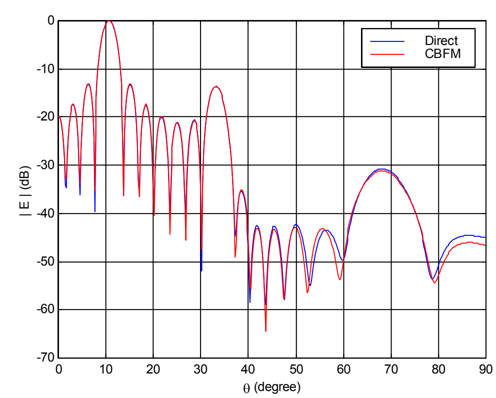

Fig. 18. H-plane far field pattern of 7 x 7 array of waveguide-with-FSS macrocell (441 waveguide elements).

We close this section with one final comment on the slight differences between the direct and CBFM results for wide angles that are present in the pattern plots appearing in both Figs. 18 and 19. Our experience shows that, for large problems being simulated directly, it becomes necessary to extend the size of the computational domain in the vertical direction in order to reduce the spurious reflections from the top surface of the perfectly matched layer (PML) boundary that

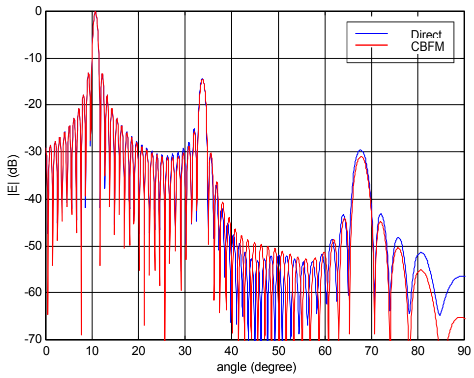

Fig. 19. H-plane far field pattern of 21 x 21 array of waveguide-with-FSS macrocell (3969 waveguide elements).

introduce errors at wide scan angles. Obviously, moving the PML boundary further away increases the problem size even more in the direct simulation case, and often renders the problem unmanageable. However, we note that the levels of these spurious reflections from the PML boundaries are much lower in the CBFM, since the simulation is carried out for a much smaller geometry than in the direct simulation. In fact, we have found that, for large problems, the CBFM results can be more accurate than the direct solution, especially at wide angles.

V. CONCLUSION

In this paper we have presented a novel approach, based on the Characteristic Basis Function Method (CBFM), for solving large phased array problems that may be covered with an FSS radome. A key feature of the method is that it builds on the solution of a moderate-size problem, which is manageable in terms of CPU memory and time, to construct the solution of a much larger problem, with little extra computational effort. Numerous representative examples have been included in the paper to validate the proposed approach, both for phased arrays and array-radome composites. Although not discussed in this paper, the CBFM has been useful for solving large-body scattering problems as well, including radar targets and antennas mounted on complex platforms.

References

[1] Yee, K. S. "Numerical solution of initial boundary value problems involving Maxwell's equation in isotropic media," *IEEE Trans. Antennas and Propagation*, Vol. 14, 1966, pp. 302-307.

[2] R. Mittra, "A Proposed New Paradigm for Solving Scattering Problems Involving Electrically Large Objects using the Characteristic Basis Functions Method," *Proceedings of the International Conference on Electromagnetics in Advanced Applications (ICEAA)* 2003, Turin, Italy, pp. 621-624, Sep. 2003.

[3] R. Mittra, "Solution of Large Array and Radome Problems using the Characteristic Basis Function Approach," *IEEE Antennas & Propagation Society International Symposium/URSI*, Columbus, Ohio, June 2003.

[4] H. E. AbdEl-Raouf, R. Mittra, and J.-F. Ma, "Solving Very Large EM Problems (109 DoFs or Greater) Using the MPI-CBFDTD Method," *IEEE International Symposium on Antennas and Propagation and USNC/URSI National Radio Science Meeting* (AP-S'05), July 3-8, 2005.

[5] T. Su, L. Ma, N. Farahat, and R. Mittra, "Modeling of a Large Slotted Waveguide Phased Array Using the FDTD and Characteristic Basis Function (CBF) Approaches," URSI'03, June 22-27, 2003.

Nader Farahat is Associate Professor in the Electrical Engineering Department of Polytechnic University of Puerto Rico. He is also adjunct research associate at the Pennsylvania State University.

Neng-Tien Huang recently completed his Ph.D. program in Electrical Engineering at the Pennsylvania State University, and is currently serving as an intern at Intelligent Automation Incorporated (IAI) in Rockville, Maryland.

Raj Mittra is Professor in the Electrical Engineering department of the Pennsylvania State University and the Director of the Electromagnetic Communication Laboratory. He is also the President of RM Associates, which is a consulting organization that provides services to industrial and governmental organizations, both in the U. S. and abroad.